Diindolylmethane Inhibits Cervical Dysplasia, Alters Estrogen Metabolism, and Enhances Immune Response in the K14-HPV16 Transgenic Mouse Model

Daniel W. Sepkovic,[1] Johann Stein,[2] Antoine D. Carlisle,[1] H. Barbara Ksieski,[1] Karen Auborn,[3] and H. Leon Bradlow[1]

[1]The David and Alice Jurist Institute for Research and [2]Piasek Biotech, Inc., Hackensack University Medical Center, Hackensack, New Jersey and [3]The Feinstein Institute for Medical Research, North Shore Long Island Jewish Health System, Manhasset, New York

Abstract

This study was designed to establish whether 3,3′-diindolylmethane (DIM) can inhibit cervical lesions, alter estrogen metabolism in favor of C-2 hydroxylation, and enhance immune function in the K14-HPV16 transgenic mouse model. Mice were bred, genotyped, implanted with E_2 pellets (0.25 mg/90-day release) under anesthesia, and divided into groups. Wild-type and transgenic mice were given either AIN76A diet alone or with 2,000 ppm DIM for 12 weeks. Blood and reproductive tracts were obtained. Blood was analyzed for estrogen metabolites and IFN-γ. The cervical transformation zone was sectioned and stained for histology. Estradiol C-2 hydroxylation and serum IFN-γ levels were significantly increased over controls in wild-type and transgenic mice receiving DIM. In wild-type mice without DIM, hyperplasia of the squamous epithelium was observed. Wild-type mice fed DIM displayed a normal thin epithelium. In transgenic mice without DIM, epithelial cell projections into the stroma (papillae) were present. An additional degree of nuclear anaplasia in the stratum espinosum was observed. Dysplastic cells were present. Transgenic mice fed DIM displayed some mild hyperplasia of the squamous epithelium. DIM increases estrogen C-2 hydroxylation in this model. Serum INF-γ was increased, indicating increased immune response in the DIM-fed animals. Histopathology showed a marked decrease in cervical dsyplasia in both wild-type and transgenic mice, indicating that DIM delays or inhibits the progression from cervical dysplasia to cervical cancer. Using the K14-HPV16 transgenic mouse model, we have shown that DIM inhibits the development of E6/E7 oncogene–induced cervical lesions. (Cancer Epidemiol Biomarkers Prev 2009;18(11):2957–64)

Introduction

Although cervical cancer incidence and mortality rates have declined in the United States over the past three decades, the disease remains a serious national and international health issue. Incidence rates for Hispanic women are higher than those for non-Hispanic women. Although the mortality rate for African American women has declined more rapidly than the rate for Caucasian women, the African American mortality rate continues to be more than double that of Caucasians (1).

The human papillomavirus (HPV) is recognized as the major cause of cervical cancer. In 2006, an estimated 10,000 women in the United States were diagnosed with this type of cancer and nearly 4,000 will die from it. Cervical cancer strikes nearly half a million women each year worldwide, claiming a quarter of a million lives (2).

HPVs are divided into "low-risk" and "high-risk" (types that are more likely to lead to the development of cancer) viruses. Both types of HPV can cause the growth of abnormal cells, but generally only the high-risk types of HPV may lead to cancer. Sexually transmitted, high-risk HPVs include types 6, 11, 16, 18, and a few other less frequent variants (3).

Early studies by Wattenberg have shown that compounds present in cruciferous vegetables had potent anticancer activity (4). Chemical analysis indicated that the activity could be accounted for by two classes of compounds, the indole derivatives originating from glucobrassinin and the various isothiocyanates, including phenylhexylisothiocyanate as gluconasturtin and sulforaphane derived from glucoraphanin. Our focus is on the indoles. The initial compound released from glucobrassinin by the action of the enzyme myrosinase is indole-3-carbinol (I3C), a compound that has proved to be highly unstable both *in vitro* and *in vivo* (5).

Most early studies were carried out using I3C either as an additive in cell culture studies or given p.o. in animal and human studies without any concern for its stability. In animal studies, it was shown to have activity against breast tumor formation (6, 7) and against endometrial tumors (8). In cell culture studies and in human studies, I3C/3,3′-diindolylmethane (DIM) increased 2-hydroxylation of estradiol and decreased 16α-hydroxylation (9, 10). This change was correlated with its antitumor activity.

I3C given p.o. is almost immediately converted to a number of condensation products in the stomach in varying proportions, depending upon the exact pH (11). These include a dimer, DIM; trimers including the linear trimer

Received 7/13/09; revised 8/24/09; accepted 9/11/09; published OnlineFirst 10/27/09.
Grant support: NIH grant 1R01CA136847.
Requests for reprints: Daniel W. Sepkovic, The David and Alice Institute for Research, Hackensack University Medical Center, 30 Prospect Avenue, Hackensack, NJ 07601. Phone: 917-673-0829; Fax: 201-457-1882. E-mail: dsepkovic@humed.com

doi:10.1158/1055-9965.EPI-09-0698

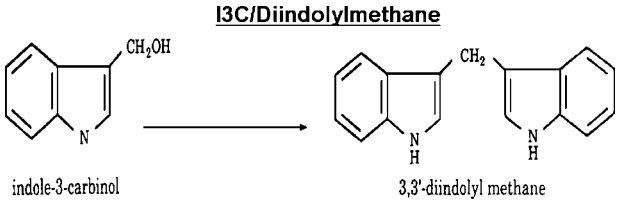

Figure 1. Chemical structure of I3C/DIM. Indole-3-carbinol is derived from the glucosinolate, glucobrassicin that is present in cruciferous vegetables. Upon contact with the acid environment of the stomach, several acid condensation products are formed. The primary acid condensation product is DIM.

{LTR, [2-(indol-3-ylmethyl) indol-3-yl] indol-3-ylmethane} and the cyclic trimer (CTR, 5,6,11,12,17,18-hexahydrocyclonal [1,2-b: 4,5-b':7,8-b]); the closed ring dimer indolocarbazole (ICZ, indolo[3,2-b]carbazole); and ascorbigen, the condensation product of I3C and ascorbic acid (12). Although DIM predominates, variable amounts of the others are also formed depending on the exact pH in the stomach or in the media. At least one of the other compounds (LTR) has a proestrogenic response and would not be protective (13, 14). The chemical structures of I3C and the primary acid condensation product DIM are given in Fig. 1.

Even in neutral conditions (pH 7.0-7.4) in tissue culture media, I3C is rapidly converted to DIM (10). Attempts to measure plasma I3C after p.o. administration of I3C to mice showed only a transient minimal blood level of I3C for only a few minutes, when 250 mg/kg was given (6). DIM is a useful preventive for cervical-vaginal cancer, as well as other cancers with a papillomavirus component. DIM alters the phase I metabolism of estradiol in favor of C-2 hydroxylation pathways and away from C-4 or C-16 hydroxylation (12, 15-18). C-16 hydroxylation produces 16α-hydroxyestrone, an endogenous carcinogen that is a promoter of HPV 16 and 18 proliferation (12, 15). DIM, by altering the directional pathway of estrogen metabolism and probably through other nonestrogenic effects, induces viral dormancy. DIM suppresses viral infection in children with recurrent respiratory papillomatosis, an HPV induced disease state (19, 20).

HPV infection activates cervical intraepithelial neoplasia (CIN), which progresses through various stages to cervical cancer. E6 and E7 exons from viral DNA interfere with the host cell control of transcription and the cell cycle. Normal cell division is regulated by two tumor suppressor gene products, Rb (retinoblastoma protein), which promotes smooth transition through the cell cycle, and P53, which stops cell division when DNA is damaged promoting DNA repair. The viral protein E7 binds to Rb and causes uncontrolled cell reproduction, which is one of the definitions of a malignant cell. The E6 viral protein binds to P53 and the protein inactive. E6 also activates telomerase, which promotes malignancy as the mutant cells continue to reproduce uncontrollably (21).

DIM disrupts several stages of HPV proliferation that influence the initiation and progression from cervical dysplasia to cervical cancer. Carter et al. and Yuan et al. have shown that DIM specifically inhibits proliferation of viral transcripts E6 and E7 in human keratinocytes and in CaSki cells (22, 23). DIM can induce a G_1 cell cycle arrest in MCF-7 cells, which is accompanied by inhibition of cyclin-dependent kinase expression (24). DIM inhibits cell adhesion, spreading,

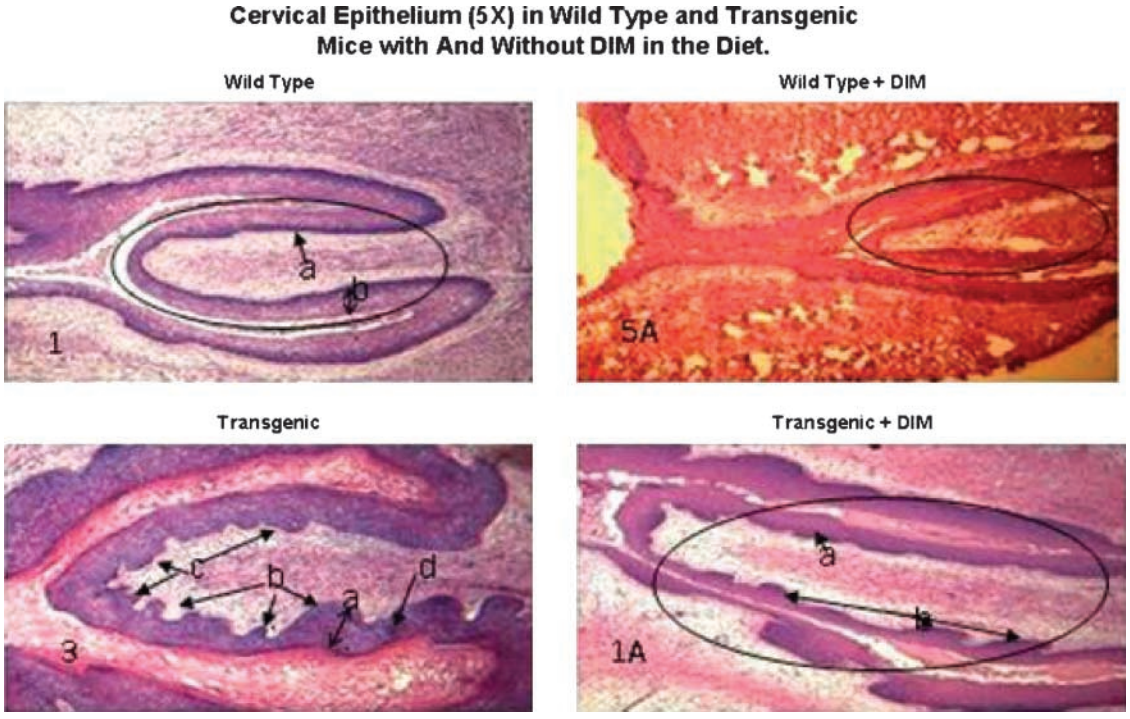

Figure 2. Cervical epitheliun (5×) in wild-type and transgenic mice with and without DIM in the diet. DIM decreases cell proliferation and papillae invasion and prevents thickening of the cervical epithelium in both wild-type and K14-HPV 16 transgenic mice. After 12 wk of DIM consumed in the diet.

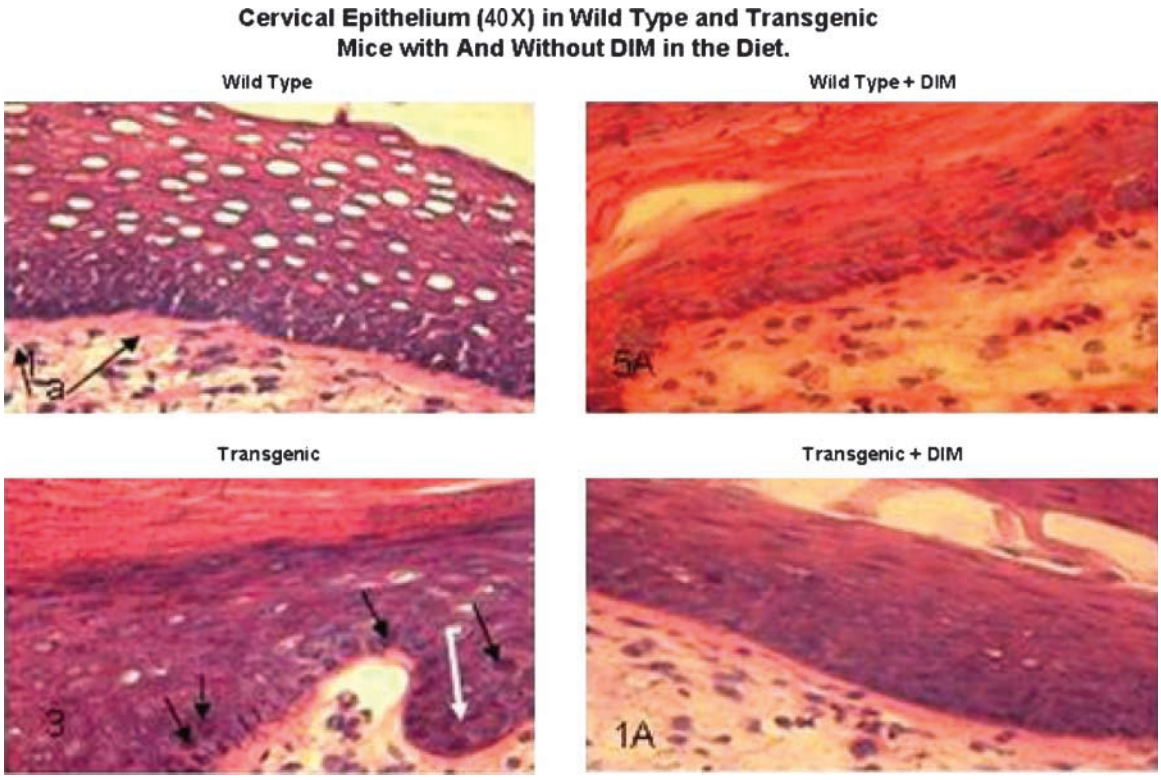

Figure 3. Cervical epitheliun (40×) in wild-type and transgenic mice with and without DIM in the diet. In the wild-type specimen, hyperplasia of the squamous epithelium was observed (a). Wild type plus DIM displayed a normal thin epithelium. In the transgenic specimen, epithelial cell projections into the stroma are apparent (papillation, arrow). Some cells exhibit an additional degree of nuclear anaplasia (white arrow) in the stratum espinosum (out of the stratum basale). Epithelial cells projected into the stroma are displayed. Dysplastic cells are present (arrows). The specimen for the transgenic mouse with DIM displayed some mild hyperplasia of the squamous epithelium.

and invasion associated with the upregulation of PTEN (a tumor suppressor gene) and E-cadherin (a regulator of cell-cell adhesion) in T-47-D human breast cancer cells (25). These mechanisms may also apply to the initiation and progression via increasing severity of CIN to cervical carcinoma. Additionally, DIM prevents PTEN loss *in vivo* in the K14HPV16 transgenic mouse model (26).

DIM elevates four key cytokines *in vivo*: IFN-γ, granulocyte colony-stimulating factor, interleukin-12 (IL-12), and IL-6. IFN-γ is an indicator of overall immune response (27, 28). Granulocyte colony-stimulating factor is responsible for WBC production in the body. IL-6 is responsible for the body's direct antibacterial response. IL-12 stimulates the growth and function of T cells that help to fight off pathogens, such as viral infections.

Reduction in the severity of CIN and, in some cases, the complete elimination of cervical dysplasia indicate that HPV16 oncogene expression becomes latent after continued DIM administration. The objective of this study is to monitor changes in estrogen metabolism, IFN-γ levels, and cervical histology in mice after receiving DIM in the diet and to compare these objective biomarkers with respective controls.

Materials and Methods

The K14-HPV16 mouse model is well established and is frequently used in studies involving cervical dysplasia and cervical cancer (29). Cervical neoplasia and cancer are linked to persistent infection of "high-risk" HPV viral types, where E6 and E7 oncogenes have enhanced affinity for cellular proteins, controlling a collection of functions necessary for neoplastic progression or growth and spread of malignancies. The K14-HPV16 mouse model is transgenic for the entire HPV16 early region under control of the human keratin-14 promoter and expresses HPV16 E6 and E7 oncogenes in basal squamous epithelial cells.

Tumorigenesis in this model is hormone dependent. Chronic estradiol treatment at 0.1 to 0.25 mg/90 d induces invasive squamous cancers in the vulva, vagina, and outer cervix of K14-HPV16 mice. None of the tumors are metastatic. At low estradiol dose (0.05 mg/90 d), squamous cancers are almost exclusively localized to the transformation zone situated between the upper cervix and lower uterus. Epithelial dysplasia and metaplasia are observed after 4 mo of estradiol treatment, leading to high-grade dysplasia and multifocal carcinomas by 6 mo (30).

Breeder pairs were kindly provided by the National Cancer Institute Mouse Repository [Mouse Models of Human Cancers Consortium (MMHCC), Frederick, MD]. After arrival, the mice were quarantined for as long as deemed necessary by the veterinarian based on serologic testing and results. The mice were housed four per cage. These cages have sterile microisolator tops. They were fed irradiated AIN-76A diet and given sterile water via sterile

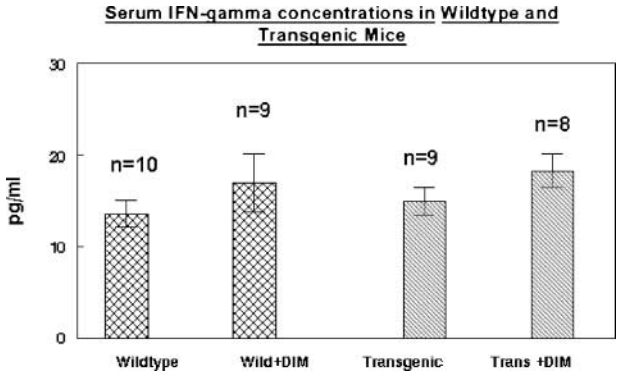

Figure 4. Serum IFN-γ levels in wild-type and transgenic mice receiving 2,000 ppm DIM continuously in the diet. Mean serum IFN-γ concentrations were significantly higher ($P < 0.05$) in both groups that were fed 2,000 ppm in the diet when compared with mice receiving diets that did not contain DIM.

water bottles. The animals were given daily health checks, which included a pain scale form.

Breeding began during quarantine. The hemizygote K14-HPV16 was bred with the FVB wild type to produce the first litter of pups. At weaning, the pups were to be genotyped. Those mice exhibiting the E6-E7 exon (K14-HPV16 positive) were bred with FVB wild type to generate progeny for the experimental protocols. Once pregnancy was determined, the females were separated into individual cages for parturation and rearing. All females (K14-HPV16 and FVB wild type) were trochar implanted with E_2 pellets (0.25 mg/90-d release; Innovative Research of America, Sarasota, FL) at weaning under anesthesia. The Animal Resource Facility strictly follows the guidelines laid out by the Association for Assessment and Accreditation of Laboratory Animal Care International, the policies according to the Public Health Service Policy on Humane Care and Use of Laboratory Animals, and guidelines set forth by the Animal Welfare Act.

The animals were given AIN-76A mouse diet until they were divided into their respective groups. Two groups received AIN-76A mouse diet without DIM added, and two groups were given AIN-76A mouse 2,000 ppm of DIM. The diets were prepared by Land O'Lakes Purina Feed, LLC (TestDiet Division).

Genotyping the Mouse Model. Mouse tail clippings were digested using proteinase K in TNES buffer at 55°C overnight. DNA was isolated using 6 mol/L NaCl and chloroform-isoamyl alcohol according to established procedures. The DNA was amplified by using primers JA7 (5′-aga act gca atg ttt gac cca cag-3′) and JA4 (5′-tct gca aca aga cat aca tcg acc gg-3″). JA7 and JA4 are MMHCC designations. The primers were provided by Invitrogen. The master mix reagents, primer combinations, and cycling conditions were provided in the FVB.Cg-Tg (KRT-HPV16)wt1Dh PCR protocol (MMHCC). The Indy Air Thermocycler was used to conduct high-speed PCR (Idaho Technologies, Inc.). The PCR products were visualized by ethidium bromide staining of 2.0% agarose gels. Each mouse was genotyped and identified as either wild type or transgenic and then grouped accordingly.

Tissue Procurement and Determination of Changes in Cervical Morphology. Mice were anesthetized, and blood was obtained by cardiac puncture. Reproductive-tracts and surrounding soft tissue and lymph nodes were dissected and immediately frozen at −80°C. The entire reproductive tract was serially sectioned, and 10 to 15 sections were collected at 75-μm intervals for H&E staining using a Cryocut 1800 Cryostat (Reichert-Jung). Examination of serial sections was done with an inverted Nikon Te300 microscope with Hoffmann contrast optics for phase microscopy, as well as bright field for H&E work. The microscope has 5×, 10×, and 40× objectives.

A histopathologic grading system for transgenic mouse cervical squamous carcinogenesis developed by Riley et al. (21) was used to classify histologic samples. This grading system is based on the established criteria for classification of human cervical neoplasia or malignancy accounting for differences between the mouse model and patients. Using this mouse cervical neoplasia grading system, CIN-I consists of a 2-fold increase in the basal/basaloid cell layers of cervical and vaginal squamous epithelia of transgenic compared with estrogen-treated nontransgenic mice. CIN II lesions contain cells with additional increases in nuclear size, degree of anaplasia, frequency, and distribution of dysplastic cells in the suprabasal layers of the squamous epithelium. Moreover, the basal aspect of the squamous epithelium is projected into papillary folds projecting into the underlying vaginal or cervical stroma. CIN III lesions contain abundant anaplastic cells, some with pronounced increases in nuclear size. CIS (high grade dysplasia) shows a pronounced degree of remodeling and undulation of the epithelial-stromal border and most of the cellular features of well-differentiated squamous carcinoma, with retention of an intact basement membrane without evidence of microinvasion on serial sections.

Assessment of Immune Response Using Serum IFN-γ Levels. Mouse IFN-γ was analyzed using serum by ELISA (eBioscience). The assay is straightforward and specific for the analyte. Appropriate controls were run in each assay, and the samples were run in triplicate.

Quantification of DIM in Serum. Extraction of DIM from Serum-100 μL of serum was diluted with 1 mL of sodium acetate buffer (pH 4.8) and 20 μL of glucuronidase (110,200 units/mL; Sigma). The solution was incubated at 40°C for 24 h. The internal standard, 4,4-dichlorodiindolylomethane (dichloro-DIM generously provided by Dr. Stephen Safe), was then added, and the

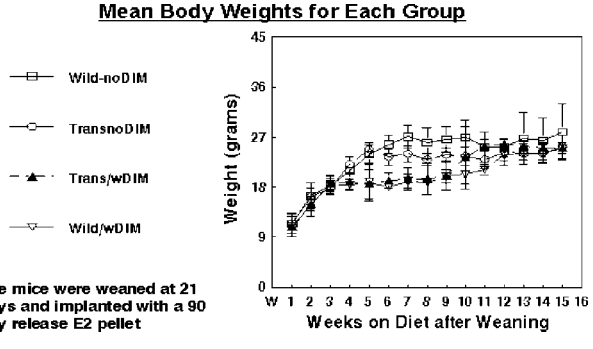

Figure 5. Mean body weights for wild type with and without 2,000 ppm DIM in the diet and transgenics with and without 2,000 ppm DIM in the diet. Mean body weights were similar for all groups.

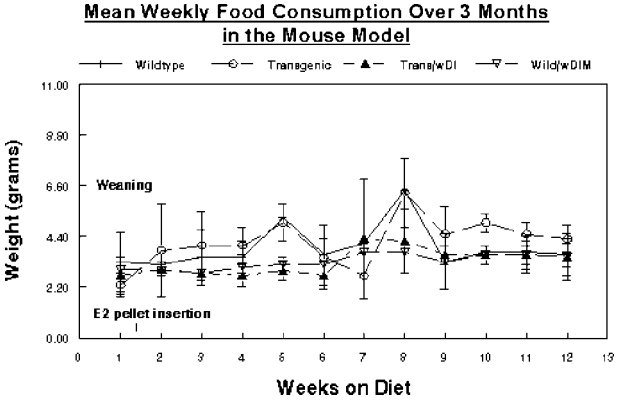

Figure 6. Mean food consumption for wild type with and without 2,000 ppm DIM in the diet and transgenics with and without 2,000 ppm DIM in the diet. Animals in both DIM groups consumed slightly less food (~5%) over the monitoring period.

sample is extracted with chloroform. Twenty microliters of dry pyridine and 80 μL of *N,O-bis*(trimethylsilyl) trifluoroacetamide catalyzed with 1% trimethyl-chlorosilane (Pierce Chemical) were added, and the sample was heated to 100°C for 1 h. The sample is injected without further treatment (31). Gas chromatography–mass spectrometry (GC-MS) conditions are identical to those used for the determination of estrogen metabolites.

Determination of Estrogen Metabolites in Serum. Serum was diluted 1:1 with sodium acetate buffer (pH 4.65) and 20 μL of β-glucuronidase (110,200 units/mL, Sigma). The solution was incubated at 40°C for 24 h to deconjugate the steroids. After the addition of deuterated estradiol, each sample was thoroughly vortexed and extracted with chloroform. The chloroform extract was evaporated to dryness under nitrogen. The residue was derivitized with 10 μL of dry pyridine and 40 μL of *bis*(trimethylsilyl)-trifluoroacetamide, vortexed, and allowed to react at room temperature overnight. One microliter of each sample was injected into GC-MS without further treatment.

GC-MS Conditions. An Agilent Technologies 6980N gas chromatograph equipped with an Agilent 5973 mass selective detector, an Agilent 7683 injector, and an HP G1701CA MSD Chemstation was used for the analysis of estradiol and selected metabolites. The injection port was equipped with a split/splitless capillary inlet system and a silanized glass insert. The temperature of the injection port was maintained at 300°C, the interface at 270°C, and the ion source at 280°C. The ionization energy was 70 eV. The carrier gas was helium at a flow rate of 1 mL/min. Separations were carried out using a Hewlett-Packard Ultra 2 capillary column with cross-linked 5% phenyl-methyl silicone (25 m × 0.2 mm × 0.33 μm film thickness). The oven temperature was increased from 60°C to 260°C at 40°C/min then at 1°C/min to 280°C.

Under selected ion monitoring, the following mass ions and GC elution times of trimethylsilylated estrogens were monitored: estrone (E_1) m/z 342, estradiol (E_2) m/z 416, deuterated estradiol (d_4E_2) m/z 420, 2-hydroxyestrone (2-OHE_1) m/z 430, 4-hydroxyestrone (4-OHE_1) m/z 430, 16α-hydroxyestrone (16α-OHE_1) m/z 286 and 430, and estriol (E_3) m/z 504. [2,4,16α,16β-^{2}H4]; estradiol was synthesized in our laboratory according to the method of Dehennin et al. and used as an internal standard. Each of the above steroids was quantified using a six-point calibration curve that ranged from 1 to 100 ng (32-35).

Results

Histopathology. DIM decreases cell proliferation and papillae invasion and prevents thickening of the cervical epithelium in both wild-type and K14-HPV16 transgenic mice. Histopathology of the cervico-uterine transformation zone in wild-type and transgenic mice that have received either the normal mouse diet or the diet enriched with 2,000 ppm of DIM for 12 weeks are presented in Fig. 2.

The wild-type specimen has an oval encircling the cervix. Thickened epithelium and mild hyperplasia (b) are apparent. The stratum basal was well demarcated [deep purple (a)]. Papillae (projections of the collagen layer into the epithelium) were absent. The wild type plus DIM specimen shows a normal epithelial thickness. A few mild papillae were also present.

In the transgenic specimen, increased squamous hyperplasia (a) was observed. Epithelial papillomatosis (b) was apparent. Anaplastic squamous epithelial cells were observed at the stratum basale (c). Dysplastic cells (d) in the epithelium at the level of stratus espinosum and/or granular were observed. No glandular hyperplasia or keratin pearls were observed in any of the analyzed specimens.

In the transgenic plus DIM specimen, the oval line represents the cervix. Increased squamous hyperplasia (a) and epithelial papillae (b) were present. There are 41% less epithelial papillae projecting into the stroma in the DIM-treated transgenic mice when compared with transgenic not receiving DIM in the diet over a 12-week period. Dysplastic cells in the epithelium at the level of stratus espinosum and/or granular were not observed at this magnification. No glandular hyperplasia or keratin pearls were observed in any of the analyzed specimens.

The cervical region was examined at higher magnification (Fig. 3). In the wild-type specimen, hyperplasia of the squamous epithelium was observed (a). This corresponds to CIN-I in the histopathologic grading system of Riley et al. (31). The wild type plus DIM slide displayed a normal thin epithelium. In the transgenic specimen,

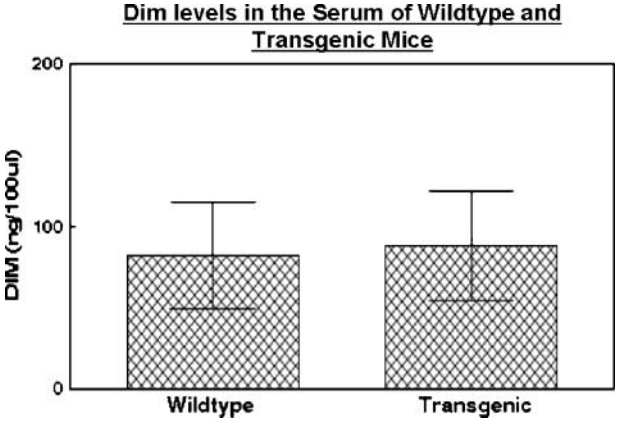

Figure 7. DIM concentrations in wild-type and transgenic mice receiving 2,000 ppm DIM continuously in the diet. DIM concentrations in serum were quantified by GC-MS using the method of Sepkovic et al. (32).

Table 1. Comparison of estrogen metabolism in wild-type and HPV transgenic mice with and without 2,000 ppm DIM in the diet

		E_1	E_2	2-OHE_1	16-OHE_1	4-OHE_1	E_3	C-2/C-16 ratio
Wild type, $n = 9$	Mean	4.7	0.8	0.9	1.9	0.0	1.5	0.5
	SD	5.0	0.5	1.0	1.5	0.1	1.5	
Wild type with DIM, $n = 7$	Mean	4.8	0.2	3.2	1.1	0.0	0.1	2.8
	SD	4.3	0.2	3.7	1.0	0.0	0.3	
Transgenic, $n = 10$	Mean	3.6	0.3	0.3	1.3	0.0	0.7	0.2
	SD	4.2	0.3	0.3	0.9	0.0	0.7	
Transgenic with DIM, $n = 10$	Mean	1.0	1.6	1.0	0.9	0.0	0.9	1.1
	SD	1.2	2.6	1.1	1.1	0.1	1.0	

NOTE: DIM increased C-2 hydroxylation of estradiol in both wild-type mouse and HPV transgenic mouse by 28% ($P < 0.05$) and 33% ($P < 0.05$), respectively.

epithelial cell projections into the stroma (papillations, arrow) were apparent. Cells with an additional degree of nuclear anaplasia (white arrow) were observed in the stratum espinosum (out of the stratum basale). Epithelial cells projecting into the stroma were displayed. Dysplastic cells were present (arrows). This corresponds to CIN-II/CIN-III in the histopathologic grading system of Riley et al. (31). The cervical transformation zone for the transgenic mouse with DIM displayed only mild hyperplasia of the squamous epithelium.

Immune Response. Mean serum IFN-γ concentrations were significantly higher ($P < 0.05$) in both groups that were fed 2,000 ppm in the diet when compared with mice receiving diets that did not contain DIM (Fig. 4). Xue et al. (28) was able to show an increase in 4 of 22 cytokines using a mouse membrane cytokine array using male C57BL/6 mice. They administered a single p.o. (30 mg/kg) dose of DIM in a C57Bl/6 male mouse model ($n = 3$), and serum was sampled at regular intervals over 24 hours. Each cytokine exhibited different kinetics with IFN-γ levels increasing after 24 hours. C57BL/6 has certain immunophenotypes that distinguish it from other inbred strains like BALB/c. The K-14 HPV 16 model used here is transgenic, and the FVB wild-type mouse may respond at greater doses of DIM. It is important to note that the study by Xue (28) used male mice. We are using estradiol-implanted females. The induction of cytokines by DIM has not been attempted previously in this model.

Mean body weights for each group for 15 weeks are presented in Fig. 5. Mean body weights were similar for all groups.

Food Consumption. Food consumption was monitored in each group (Fig. 6). These measurements were begun after weaning and E_2 pellet implantation. Animals in both DIM groups consumed slightly less food (~5%) over the monitoring period. This may be due to taste differences or possibly other factors. All groups had dietary consumption levels that were consistent with animal feeding recommendations for mice on custom purified diet (3-6 g/animal/day; ref. 36).

DIM concentrations in serum were quantified by GC-MS using the method of Sepkovic et al. (31). DIM levels in serum were not different in either of the groups receiving DIM in the diet. No DIM was found in the groups receiving mouse chow alone (Fig. 7).

Estrogen metabolites were quantified by stable isotope dilution GC-MS in the blood of wild-type and transgenic mice with and without DIM given in the diet for 12 weeks (Table 1). The results are presented as ng/100 μL serum. 2-Hydroxyestrone concentrations are significantly increased after DIM administration in both wild-type and HPV transgenic female mice. In contrast, there was no increase in 16-OHE_1 concentrations. 2-OHE_1/16-OHE_1 ratios reflect increased C-2 hydroxylation in the DIM-fed groups. 4-OHE_1 concentrations were unchanged in both wild-type and transgenic groups.

Discussion

The objective of this study was to monitor changes in estrogen metabolism, IFN-γ levels, and histopathology in mice after receiving DIM in the diet and to compare these objective biomarkers with respective controls. Using this model, we have shown that immune responses (IFN-γ levels) are significantly increased in both wild-type and HPV transgenic mice after DIM administration in the diet for 12 weeks. Although the increases in IFN-γ after DIM administration were modest, Garcia-Pineres et al. (37, 38) have shown that IFN-γ levels and the levels of other cytokines are increased after vaccination with HPV type 16 L1 virus–like particles. Our goal is to test the efficacy of vaccines in the mouse model. These vaccines contain L1 virus–like particles.

Marked changes in cervical histology were observed in the DIM-fed groups when compared with their respective controls. Estrogen metabolites were quantified by stable isotope dilution GC-MS in the blood of wild-type and transgenic mice with and without DIM given in the diet for 12 weeks. The results are presented as ng/100 μL serum. 2-Hydroxyestrone concentrations are significantly increased after DIM administration in both wild-type and HPV transgenic female mice. The C-2/C-16α hydroxylation ratio is also increased in both groups.

Yuan et al. (23) have shown that 16α-OHE_1 increased expression of HPV E6/E7 oncogenes, whereas I3C/DIM and the estrogen metabolite 2-OHE_1 abrogated the estrogen-increased expression of HPV oncogenes in Caski cells. This study provides evidence of suppressed E6/E7 oncogene expression by DIM *in vivo* through comparison of cervical histology in DIM-fed transgenic mice with respective controls. This confirms the results of a study by Jin et al. (39) wherein dietary administration of 2,000 ppm I3C for 24 weeks prevented cervical cancer in K14-HPV16 transgenic mice and reduced cervical dysplasia in FVB/n nontransgenic controls.

It should also be noted that the DIM plasma levels observed in mice in this study approximate those observed in humans given a single 1,000-mg dose of DIM (14). In the study by Jin et al. (39), which used the same transgenic mouse model as that described herein, a solid diet

containing 2,000 ppm of I3C was fed to the animals over 24 weeks without any overt signs of toxicity. As mice consume 3 g of solid food per week, the 2,000-ppm I3C–enriched diet is equivalent to a dose of 2 g I3C/kg diet or 2 mg I3C/g diet. This amount of dietary I3C could be ingested by humans who consume a diet heavily enriched in cruciferous vegetables (40, 41). This dose is comparable with the dose of DIM per day in this study.

Several pharmacokinetic studies using DIM in animals and in humans have been conducted. In mice (female CD-1 strain), Anderton et al. (13) studied I3C and DIM disposition upon p.o. administration of a dose equivalent to 7.5 mg I3C (250 mg I3C/kg body weight). Mice were sacrificed at 0 to 24 hours after dosing, after which I3C and DIM plasma and tissue (liver, kidney, lung, heart, and brain) concentrations were determined. I3C was found to be rapidly absorbed and eliminated from plasma and tissues, with plasma levels falling below detection limits by 1 h. In contrast, DIM levels in plasma were highest 2 hours after drug administration, peaking at 800 ng/mL (3.2 μmol/L). These plasma DIM levels are quite similar to those found in our own mouse model (85 ng DIM/100 μL plasma or 850 ng/mL).

Reed et al. (14) did a phase I trial in women with I3C, the precursor to DIM, where subjects received doses of I3C ranging from 400 to 1,200 mg. The only I3C-derived product found in plasma was DIM, with CMAX and AUC values that increased from 61 ng/mL (0.25 μmol/L) and 329 mg/h/L after the lower 400 mg I3C dose to 607 ng/mL (2.5 μmol/L) and 3,376 mg/h/L following the 1,000-mg dose, with no further increases noted at the higher dose. Albeit being variable, the overall DIM plasma profiles within each dosing group were qualitatively similar, with a TMAX at 2 hours and DIM levels decreasing to 20 ng/mL or less by 24 hours.

In a subsequent study, Reed et al. (42) again examined the pharmacokinetics of DIM (as well as its safety and tolerability) in a single ascending dose study but using lower doses (50-300 mg) of the agent, which was given as nutritional grade, absorption-enhanced BioResponse DIM (BR-DIM). No DIM-related adverse effects were reported at doses up to 200 mg, although at the 300-mg dose, two of six subjects reported mild nausea, headache, and/or vomiting. Analysis of plasma samples taken over the next 24 hours showed that only one of the three subjects given the 50-mg dose had detectable plasma DIM concentrations. The 100-mg dose of BR-DIM resulted in a mean CMAX of 32 ng/mL and a mean AUC of 128 mg/h/L, whereas the 200-mg dose gave a mean CMAX of 104 ng/mL and a mean AUC of 553 ng/h/mL. The 300-mg BR-DIM dose gave essentially identical CMAX and AUC values to those observed at the 200-mg dose, indicating that maximum intestinal absorption of the agent had been reached. These pharmacokinetic studies were undertaken using single-dose administration of DIM. In contrast, our study uses continuous administration of DIM contained in the mouse diet.

Taken together, the data presented here show that DIM inhibits E6/E7 oncogene expression in the HPV transgenic model through the alteration of estradiol metabolism toward C-2 hydroxylation, the enhancement of immune function, and inhibiting oncogene-induced changes in cervical histology. Yuan et al. (23) have previously shown that E6/E7 oncogene expression is suppressed by both DIM and 2-OHE_1 in CaSki cells. We have confirmed these results *in vivo*. In the mouse model, we have shown that DIM inhibits the development of E6/E7 oncogene–induced cervical lesions.

Riby et al. (27) have shown that DIM activates and potentiates IFN-γ signaling in MCF-7 cells, and Xue et al. (28) has shown that DIM stimulates murine immune function. This is the first time that estrogen metabolites and IFN-γ levels have been quantified in the K14-HPV16 mouse model after DIM consumption. The three objective biomarkers used in this study were all altered to indicate what may be viral latency. Latent viruses may permit the development of protective antibodies after HPV vaccine administration.

There is precedent for giving vaccines after viral infection. Herpes zoster results from reactivation of latent varicella-zoster virus (VZV) within the sensory ganglia. Live attenuated VZV vaccine has been given to individuals who have had herpes zoster with excellent results (43). Hope-Simpson proposed that immunity to VZV plays a pivotal role in the pathogenesis of herpes zoster, and subsequent observations support the thesis that cell-mediated immunity to VZV is a major determinant of the risk and severity of herpes zoster (44). VZV vaccine boosts cell-mediated immunity by increasing IFN-γ (45). DIM increases cell-mediated immunity through the elevation of IFN-γ as well as other cytokines mentioned above.

Disclosure of Potential Conflicts of Interest

No potential conflicts of interest were disclosed.

Acknowledgments

The costs of publication of this article were defrayed in part by the payment of page charges. This article must therefore be hereby marked *advertisement* in accordance with 18 U.S.C. Section 1734 solely to indicate this fact.

References

1. Horner MJ, Ries LAG, Krapcho M, et al. (eds). SEER Cancer Statistics Review, 1975–2006, National Cancer Institute. Bethesda (MD).
2. Division of STD Prevention. Prevention of genital HPV infection and sequelae: report of an external consultants' meeting. Atlanta (GA): Centers for Disease Control and Prevention, 1999.
3. Munoz N, Bosch FX, de Sanjosé S, et al. Epidemiologic classification of human papillomavirus types associated with cervical cancer. N Engl J Med 2003;348:518–27.
4. Loub WD, Wattenberg LW, Davis DW. Aryl hydrocarbon hydroxylase induction in rat tissues by naturally occurring indoles of cruciferous plants. J Natl Cancer Inst 1975;54:985–8.
5. De Kruif CA, Marsman JW, Venrkamp JC, Falke J. Structure elucidation of acid reaction products of indole-3carbinol: detection *in vivo* and enzyme induction *in vitro.* Chem Biol Interact 1991;80:303–15.
6. Bradlow HL, Michnovicz JJ, Telang NT, Osborne MP. Effect of dietary indole-3-carbinol on estradiol metabolism and spontaneous mammary tumors in mice. Carcinogenesis 1991;12:1571–4.
7. Grubbs CJ, Steele VE, Casebolt TL, et al. Chemoprevention of chemically induced mammary tumors. Anticancer Res 1995;15:709–16.
8. Kojima T, Tanaka T, Mori H. Chemoprevention of spontaneous endometrial cancer in female Donryku rats by dietary indole-3-carbinol. Cancer Res 1994;54:1446–9.
9. Telang NT, Kurihara H, Wong GY, et al. Preneoplastic transformation in mouse mammary tissue: identification and validation of intermediate biomarkers for chemoprevention. Anticancer Res 1991;11:1021–7.
10. Michnovicz JJ, Bradlow HL. Induction of estradiol metabolism by dietary indole-3-carbinol in humans. J Natl Cancer Inst 1990;50:947–50.
11. Preobrazhenskaya MN, Bukhman VM, Korolev AM, Efimov SA. Ascorbigen and other indole-derived compounds from Brassica vegetables and their analogs as anticarcinogenic and immunomodulating agents. Pharmacol Ther 1993;60:301–13.
12. Schneider J, Kinne D, Fracchia A, Pierce V, et al. Abnormal oxidative metabolism of estradiol in women with breast cancer. Proc Soc Acad Sci 1982;79:3047–51.

13. Anderton MJ, Manson MM, Verschoyle RD, et al. Pharmacokinetics and tissue disposition of indole-3-carbinol and its acid condensation products after oral administration to mice. Clin Cancer Res 2004;10: 5233–41.
14. Reed GA, Arneson DW, Putnam W, III, et al. Single- and multiple-dose administration of indole-3-carbinol to women: pharmacokinetics based on 3,3′-diindolylmethane. Cancer Epidemiol Biomarkers Prev 2006;15:2477–81.
15. Auborn KJ, Woodworth C, DiPaolo JA, Bradlow HL. The interaction between HPV infection and estrogen metabolism in cervical carcinogenesis. Int J Cancer 1991;49:867–9.
16. Fishman J, Schneider J, Hershcope RJ, Bradlow HL. Increased estrogen 16 α-hydroxylase activity in women with breast and endometrial cancer. J Steroid Biochem Mol Biol 1984;20:1077–81.
17. Steinberg BM, Auborn KJ. Papillomavirsuses in head and neck disease: pathophysiology and possible regulation. J Cell Biochem 1993; 17F:155–64.
18. Michnovicz JJ, Adlercreutz H, Bradlow HL. Changes in levels of urinary estrogen metabolites after oral indole-3-carbinol treatment in humans. J Natl Cancer Inst 1997;89:718–23.
19. Auborn K, Abramson A, Bradlow HL, et al. Estrogen metabolism and respiratory papillomatosis: a pilot study on dietary prevention. Anticancer Res 1998;18:4569–74.
20. Coll DA, Rosen CA, Auborn K, et al. Treatment of recurrent respiratory papillomatosis with indole-3-carbinol. Am J Otolaryngol 1997;18: 283–5.
21. Riley RR, Duensing S, Brake T, et al. Dissection of human papillomavirus E6 and E7 function in transgenic mouse models of cervical carcinogenesis. Cancer Res 2003;63:4862–71.
22. Carter TH, Liu K, Ralph W, Jr., et al. Diindolylmethane alters gene expression in human keratinocytes *in vitro*. J Nutr 2002;132:3314–24.
23. Yuan F, Chen D, Liu K, Sepkovic DW, et al. Anti-estrogen effect of Indole-3-carbinol in cervical cancer cells: implication for prevention of cervical cancer. Anticancer Res 1999;19:1673–80.
24. Cram EJ, Liu BD, Bjeldanes LF, Firestone GL. Indole-3-carbinol inhibits CDK6 expression in human MCF-7 breast cancer cells by disrupting Sp1 transcription factor interactions with a composite element in the CDK6 gene promoter. J Biol Chem 2001;276:22332–40.
25. Meng Q, Goldberg ID, Rosen EM, Fan S. Inhibitory effects of Indole-3-carbinol on invasion and migration in human breast cancer cells. Breast Cancer Res Treat 2000;63:147–52.
26. Mei Q, Anderson AE, Chen DZ, et al. Indole-3-carbinol prevents PTEN loss in cervical cancer *in vivo*. Mol Med 2005;11:59–63.
27. Riby JE, Xue L, Chatterji U, et al. Activation and potentiation of interferon-(γ) signaling by 3,3′-diindolylmethane in MCF-7 breast cancer cells. Mol Pharmacol 2006;69:430–9.
28. Xue L, Pestka J, Maoxiang L, et al. 3,3-Diindolylmethane stimulates murine immune function *in vitro* and *in vivo*. J Nutr Biochem 2008; 19:336–44.
29. Arbeit JM, Munger K, Howley PM, Hanahan D. Progressive squamous epithelial neoplasia in K14-human papillomavirus type 16 transgenic mice. J Virol 1994;68:4358–68.
30. Arbeit JM, Howley PM, Hanahan D. Chronic estrogen-induced cervical and vaginal squamous carcinogenesis in human papillomavirus type 16 transgenic mice. Proc Natl Acad Sci U S A 1996;93:2930–5.
31. Sepkovic DW, Bradlow HL, Bell M. Quantitative determination of 3,3′-diindolylmethane in the urine of individuals receiving indole-3-carbinol. Nutr Cancer 2002;41:57–63.
32. Sepkovic DW, Bradlow HL, Michnovicz J, et al. Catechol estrogen production in rat microsomes after treatment with indole 3 carbinol, ascorbigen, or β napthaflavone: a comparison of stable isotope dilution gas chromatography mass spectrometry and radiometric methods. Steroids 1994;59:318–23.
33. Dehennin L, Reiffsteck A, Scholler R. Simple methods for the synthesis of twenty different highly enriched deuterium labelled steroids suitable as internal standards for isotope dilution mass spectrometry. Biochem Mass Spectrom 1980;7:493–9.
34. Raju U, Sepkovic D, Dixon JM, et al. Estrone and estradiol metabolism *in vivo* in human breast cysts. Steroids 2000;65:883–8.
35. Jellnick PH, Makin HLJ, Sepkovic DW, Bradlow HL. Influence of indol carbinols and growth hormone on the metabolism of 4-androstenedione by rat liver microsomes. J Steroid Biochem Molec Biol 1993;46: 791–8.
36. Guide for the Care and Use of Laboratory Animals. Institute of Laboratory Animal Resources. Commission on Life Sciences. National Research Council. National Academy Press, Washington (DC): 1996.
37. García-Piñeres A, Hildesheim A, Dodd L, et al. Cytokine and chemokine profiles following vaccination with human papillomavirus type 16 L1 virus-like particles. Clin Vaccine Immunol 2007;14:984–9.
38. García-Piñeres AJ, Hildesheim A, Dodd L, et al. Gene expression patterns induced by HPV-16 L1 virus-like particles in leukocytes from vaccine recipients. J Immunol 2009;182:1706–29.
39. Jin L, Qi M, Chen DZ, et al. Indole-3-carbinol prevents cervical cancer in human papilloma virus type 16 transgenic mice. Cancer Res 1999; 59:3991–7.
40. Scones K, Heaney RK, Fenwick GR. An estimate of the mean daily intake of glucosinolates from cruciferous vegetables in the UK. J Sci Food Agric 1984;35:712–20.
41. Lewis J, Fenwick GR. Glucosinolate content of Brassica vegetables: analysis of twenty-four cultivars of calabrese (green sprouting broccoli, Brassica oleracea L. var. botrytis subvar. cymosa Lam.). Food Chem 1987;25:259–68.
42. Reed GA, Sunega JM, Sullivan DK, et al. Single-dose pharmacokinetics and tolerability of absorption-enhanced 3,3′-diindolylmethane in healthy subjects. Cancer Epidemiol Biomarkers Prev 2008;17:2619–24.
43. Oxman N, Levin MJ, Johnson GR, et al. A vaccine to prevent herpes zosterand postherpetic neuralgia in older adults. New Engl J Med 2005;52:2201–84.
44. Hope-Simpson RE. The nature of herpes zoster: a long-term study and a new hypothesis. Proc R Soc Med 1965;58:9–20.
45. Levin MJ, Smith JG, Kaufhold RM, et al. Decline in varicella-zoster virus (VZV)-specific cell-mediated immunity with increasing age and boosting with a high-dose VZV vaccine. J Infect Dis 2003;188: 1336–44.